

Article

Hybrid Whale and Gray Wolf Deep Learning Optimization Algorithm for Prediction of Alzheimer's Disease

Chitradevi Dhakhinamoorthy ¹, Sathish Kumar Mani ², Sandeep Kumar Mathivanan ³, Senthilkumar Mohan ³, Prabhu Jayagopal ³, Saurav Mallik ^{4,5,*} and Hong Qin ^{6,*}

¹ Department of Computer Science and Engineering, Hindustan Institute of Technology and Science, Chennai 600016, India

² Department of Computer Applications, Hindustan Institute of Technology and Science, Chennai 600016, India

³ School of Information Technology and Engineering, Vellore Institute of Technology, Vellore 632014, India

⁴ Department of Environmental Health, Harvard T.H. Chan School of Public Health, Boston, MA 02115, USA

⁵ Department of Pharmacology & Toxicology, The University of Arizona, Tucson, AZ 85721, USA

⁶ Department of Computer Science and Engineering, University of Tennessee at Chattanooga, Chattanooga, TN 37403, USA

* Correspondence: smallik@hsph.harvard.edu or sauravmtech2@gmail.com or smallik@arizona.edu (S.M.); hong-qin@utc.edu (H.Q.)

Abstract: In recent years, finding the optimal solution for image segmentation has become more important in many applications. The whale optimization algorithm (WOA) is a metaheuristic optimization technique that has the advantage of achieving the global optimal solution while also being simple to implement and solving many real-time problems. If the complexity of the problem increases, the WOA may stick to local optima rather than global optima. This could be an issue in obtaining a better optimal solution. For this reason, this paper recommends a hybrid algorithm that is based on a mixture of the WOA and gray wolf optimization (GWO) for segmenting the brain sub regions, such as the gray matter (GM), white matter (WM), ventricle, corpus callosum (CC), and hippocampus (HC). This hybrid mixture consists of two steps, i.e., the WOA and GWO. The proposed method helps in diagnosing Alzheimer's disease (AD) by segmenting the brain sub regions (SRs) by using a hybrid of the WOA and GWO (H-WOA-GWO, which is represented as HWGO). The segmented region was validated with different measures, and it shows better accuracy results of 92%. Following segmentation, the deep learning classifier was utilized to categorize normal and AD images. The combination of WOA and GWO yields an accuracy of 90%. As a result, it was discovered that the suggested method is a highly successful technique for identifying the ideal solution, and it is paired with a deep learning algorithm for classification.

Keywords: Alzheimer's disease (AD); brain sub regions; deep learning (DL); metaheuristic optimization techniques; Mini-Mental State Examination (MMSE) score

MSC: 46N10; 49Q10; 78M50



Citation: Dhakhinamoorthy, C.; Mani, S.K.; Mathivanan, S.K.; Mohan, S.; Jayagopal, P.; Mallik, S.; Qin, H. Hybrid Whale and Gray Wolf Deep Learning Optimization Algorithm for Prediction of Alzheimer's Disease. *Mathematics* **2023**, *11*, 1136. <https://doi.org/10.3390/math11051136>

Academic Editor: Jianjun Paul Tian

Received: 18 January 2023

Revised: 14 February 2023

Accepted: 21 February 2023

Published: 24 February 2023



Copyright: © 2023 by the authors. Licensee MDPI, Basel, Switzerland. This article is an open access article distributed under the terms and conditions of the Creative Commons Attribution (CC BY) license (<https://creativecommons.org/licenses/by/4.0/>).

1. Introduction

Dementia is a type of memory impairment that affects around 50 million individuals globally today. Alzheimer's disease (AD) is a degenerative illness characterized by the formation of amyloid proteins in brain cells. An increase in amyloid protein levels induces cell death and impairs signal transmission. AD is an increasing public health problem among developed countries [1]. It can be characterized by impaired intellectual functioning, which interferes with day-to-day activities or personal relationships. The impairment comprises social behavior, memory loss, thinking, and language problems. Aging is the major factor causing AD, which mainly affects people above the age of 65 years [2]. CSF-containing ventricle channels are significantly expanded in Alzheimer's disease patients [1,2]. The GM,

CC, WM, HC, and ventricle are the biomarkers to diagnose AD. Because of the location of the medial temporal lobe, variations in the ventricular shape lead to changes in GM (MTL). Ventricle changes are utilized to calculate the rates of hemispheric atrophy. The quantity of neurofibrillary tangles and the degree of senile plaque deposition in nerve cells are significantly connected to the ventricular volume, which causes GM and WM shrinkage [2]. Tissue loss usually starts in the gray matter and moves to the white matter, corpus callosum, and hippocampus. A rapid loss of tissue signals the early stages of Alzheimer's disease. Unmyelinated and myelinated neurons are both included in WM and GM. GM is composed of two components: neural connections and processing. GM is made up of a large number of cells that are situated in WM. WM serves as an information highway by connecting GM with the rest of the body components. The CC is a brain subregion that links the cerebral hemispheres, specifically the left and right hemispheres, and assists in communication between them. Apart from these entire regions, one of the major biomarkers for AD is the HC since it is completely responsible for creating new memories and recovering old ones. The primary function of the HC is to retain information in the long-term memory bank and to advance spatiotemporal communication during sleep. Tissue loss is often greater in the HC area than in the other brain subregions. Changes in the structure of the brain's subregions, especially the GM, WM, CC, ventricle, and HC, are diagnostic markers for Alzheimer's disease. However, it has been demonstrated that the HC area is more important than the other regions in diagnosing AD due to its direct link to memories [3–5]. As a result, the segmentation of brain SRs is an essential step in distinguishing between normal and AD brains. Currently, the holding technique is a prominent method for image segmentation. To differentiate between normal and Alzheimer's disease brain tissues, SRs such as the GM, WM, CSF, ventricle, CC, and HC must be segmented. For image segmentation, thresholding approaches have been classified as bi-level and multilevel. Although bi-level thresholding can be applied to normal images, it is computationally exorbitant [6,7]. Multilevel thresholding, on the other hand, may segment complicated pictures. The optimization approach can then be used to solve the disadvantages of bi-level thresholding strategies. The primary goal of applying optimization techniques is to tackle tough issues in a limited amount of time and with limited resources.

There are various problems characterized as optimization problems in real time. If complexity increases, the need for optimization methods also increases. In the initial stage, mathematical techniques were used to optimize these problems, and then heuristic optimization methods such as genetic algorithms (GAs) were proposed to simulate Darwinian evolution [8]. Next, bird behavior was mimicked by using Particle Swarm Optimization (PSO) [9]. These two algorithms have been upgraded and applied in different areas [10,11]. Additionally, swarm intelligence methods such as ant lion optimization (ALO) [12], the whale optimization algorithm (WOA) [13], moth–flame optimization (MFO) [14], the dragonfly algorithm (DA) [15], etc., have been developed to solve many different problems. Similarly, various authors have introduced different algorithms, such as the monarch butterfly optimization algorithm (MBO) [16], the Enhanced Slime Mold Algorithm (SMA) [17], Runge–Kutta threshold segmentation [18], etc., for image segmentation, and they have produced better results. All of the above swarm intelligence algorithms mimic nature. Sometimes, metaheuristic algorithms will have limitations in obtaining optimal solutions due to poor exploration and exploitation phases [19]. In this situation, there is a need to apply hybrid methods to achieve the highest performance. Classification is crucial in distinguishing between normal control (NC) and AD pictures. Various categorization approaches have been presented by various authors, including Self-Organizing Maps (SOMs), neural networks (NNs), K-Nearest Neighbors (KNN), Support Vector Machines (SVMs), and others. These algorithms use feature extraction and feature reduction approaches to operate with previously selected features. Deep learning, on the other hand, does not require the preselection of features for categorization because it contains a collection of layers to perform all of these processes during the categorization process [20].

Initially, the presented work started with the acquisition of images, which were collected from Chettinad Health City. These images are real-time images, and they may have some distortion. Therefore, a preprocessing stage was implemented to lessen the complexity and improve the quality of MR images. Disease identification and brain alterations were then investigated by introducing the WOA for segmenting brain subregions. Following that, in order to increase the performance of the WOA exploration and exploitation phases, attain targeted global optimal solutions, and solve real-time, large-scale problems, this system adds the HWGO, which is a hybrid technique. With various metrics, qualitative and quantitative analyses have been used. Finally, clinical score validation was performed for clinical analysis. These overall processes will help to clinically detect normal and AD brains.

2. Literature Review

AD is a memory disorder that causes cognitive decline. According to a statistics report, nearly fifty million people are affected by AD across the world [1]. Various authors have investigated AD pathologies and biomarkers related to AD [1–5,21]. AD destroys the cells and inhibits neuronal connectivity [22]. Relevant genes have been identified in all regions to diagnose the AD region [23]. Linear tests have been conducted to measure brain atrophy in the early stages [24]. For this reason, many authors have concentrated on brain subregions, namely, the GM, WM, HC, ventricle, and CC, to diagnose AD. The relationship between HC atrophy, WM disruption, and GM hypometabolism for AD was examined by Villan et al. [25]. According to the above literature, the CC, GM, ventricle, WM, and HC brain regions are major hallmarks of AD. Hence, it is essential to segment these entire regions to analyze AD. Several methods, including clustering-based, region-based, thresholding-based, and graph-based approaches, have been used in attempts to segment the BSRs. Thresholding is a widely used approach for picture segmentation nowadays and is derived from these methodologies. In image segmentation, thresholding methods have been divided into bi-level (just two classes, such as the background and object, with the same threshold) and multilevel (pixels with several classes). Normal photos can employ bi-level thresholding, although it is computationally expensive. Multilevel thresholding, however, has the ability to segment complex images [6]. In order to handle challenging problems within time and resource constraints, multilevel thresholding has been created to overcome the drawbacks of bi-level thresholding techniques. The metaheuristic optimization technique is the most popular method for segmentation and has been used by many researchers in the past few decades due to its flexibility, simplicity, robustness, and so on [26]. The most famous metaheuristic algorithms include Bacterial Foraging Optimization (BFO) [27], GA [28], Artificial Bee Colony Optimization (ABC) [29], moth–flame optimizer (MFO) [30], Ant Colony Optimization (ACO) [31], Particle Swarm Optimization (PSO) [9], Cuckoo Search (CS) [32], and so on. Most of the above-mentioned techniques become stuck in the local optimal solution, and this reduces the quality of segmentation. Hence, this system introduced a hybrid method with the combination of the WOA and GWO to increase the exploration and exploitation stages. GWO is a metaheuristic optimization algorithm that is inspired by the standard leadership characteristics of hunting. Similarly, the WOA replicates humpback whales' natural behavior. The WOA is a nature-inspired optimization technique that mimics the biological behavior of humpback whales. These whales are mostly found in groups, and they are experienced in special hunting methods, such as the bubble-net feeding strategy [33]. The main difference between the WOA and GWO is that the WOA employs a spiral to replicate a bubble net to hunt/chase the prey, whereas GWO simulates hunting by selecting a random search agent to find/chase the prey. As a result, the hybrid WOA and GWO optimization approach has been developed to increase the WOA performance and locate global optima. Korashy et al. applied a hybrid WOA/GWO solution to the coordination challenge of guiding overcurrent relays [34]. Using the strengths of the WOA and GWO, improved hybrid optimization algorithms have been implemented, and global optimal solutions have been obtained [35]. The primary goal of hybridization is to increase the accuracy of separate algorithms by

combining their advantages and avoiding their disadvantages. Similarly, the WOA and GWO complemented each other to improve segmentation quality. In general, analyzing AD based on structural variation necessitates segmentation and classification processes. For the past few decades, the most widely used classification methods have been Support Vector Machines (SVMs), Radial Basis Function Networks (RBFNs), neural networks (NNs), etc., for classifying normal and AD images [35]. Generally, the classification includes four steps: (1) feature extraction, (2) feature selection, (3) feature reduction, (4) feature-based classification. It consists of multiple processes and requires more time to execute. Hence, there is a need to overcome these difficulties using the current emerging techniques for classification, such as deep learning (DL) methods, which have been used. DL is a subset of machine learning (ML), and it has a deep architecture to provide efficient classification. According to a systematic review, DL is the best classifier for neuroimaging data to classify normal and AD images [36,37]. The presented work started with image acquisition from real-time hospital images, which were preprocessed to remove non-target areas, such as the skull, skin, and muscle. This step will help to improve the quality of the images. Then, the brain's internal regions, namely, the ventricle, GM, HC, WM, and CC, are segmented using WOA and HWGO techniques. The performance was tested using several measures to compare the ground truth and segmented areas. Finally, the SR images were input to the CNN classifier, which classifies the NC and AD.

3. Proposed Framework Methodologies

This study's workflow is drawn in Figure 1, which contains five steps: data acquisition, preprocessing, segmentation, ground-truth validation, and classification.

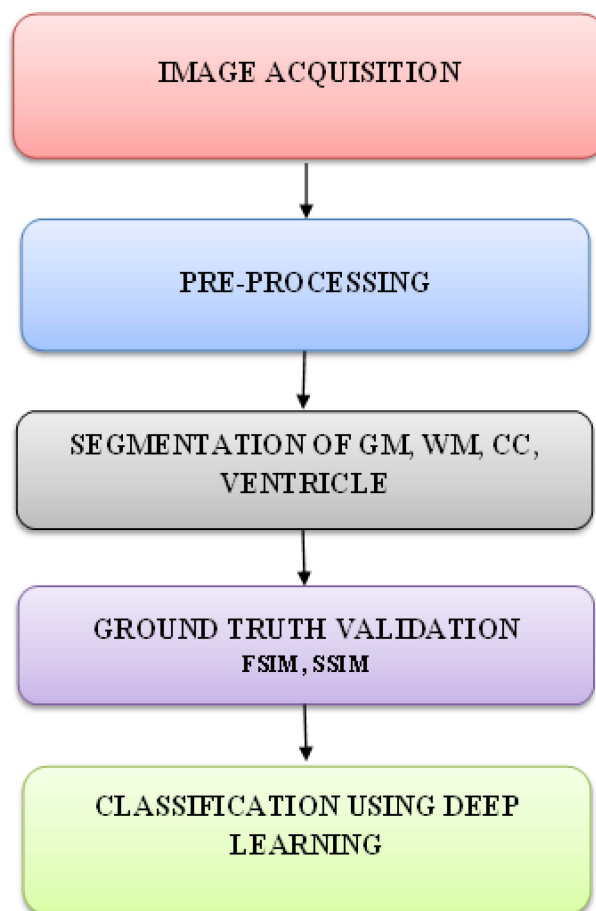


Figure 1. Overall methodology of the study.

3.1. Dataset Availability

The suggested method uses hospital brain scans to partition the brain areas into the ventricle, GM, HC, WM, and CC. T2-weighted brain MR images with axial, coronal, and sagittal slices were used. The parameters are shown in Table 1. The suggested approach segments the ventricle, HC, CC, and GM regions brain using hospital MR brain images as the input. Chettinad Hospital provided T2-weighted slices of sagittal, coronal, and axial brain MR images for the present investigation. The scanner has a 1.5-tesla standard and can produce images with 1 mm spacing, 5 mm thickness, and 256×256 resolution. A total of 100 NC and 100 AD photos were gathered, with a 60–75 age range. The ventricle and GM were segmented using axial slices. Sagittal slices were chosen to segment the CC. Similar to the previous example, coronal slices were used to segment the HC, which aids in clinical and epidemiological investigations and allows for examining both sides (the left and right) of the HC. Sagittal and axial slices cannot clearly show the HC region on both sides.

Table 1. Proposed dataset details collected from Chettinad Hospital.

Particulars	NC	AD
Number of datasets	100	100
Sex (M/F)	73/27	68/32
Age group	60.5 ± 5.5	67.5 ± 7.5
Clinical Dementia Rate (CDR)	0	1 and 2
Mini-Mental Score Examination value	26 ± 3.5	16 ± 2.5

3.2. Preprocessing

Generally, hospital images are not of good quality due to their homogeneous intensity values of both the object and background region. Since the segmentation of the brain's inner regions, especially the GM, CC, HC, ventricle, and WM, is a challenging task due to their similar intensity values, there is a need to apply preprocessing for image quality improvements. Initially, the adaptive histogram equalization approach was employed to enhance the contrast and extract distinct regions, and Otsu's thresholding method was utilized to remove undesired areas, such as the skull, skin, and muscle. Adaptive histogram equalization was used to convert each pixel using a transformation function derived from a neighboring region. Similarly, Otsu's method produces satisfactory outcomes in removing unwanted regions due to its technique of maximizing the between-class variance for extracting a better optimal solution. This approach aids in the extraction of non-brain and brain tissues with weak boundaries and equal intensities. These processes are helpful in numerous clinical applications to obtain very good accuracy, and they are key resources for brain region segmentation. The methodology of the study is presented in Figure 1.

3.3. Segmentation

The process of splitting an image into various items is known as segmentation, and it is a time-consuming procedure owing to unsatisfactory results, computational overhead, and a low generalization capability. To overcome these drawbacks, optimization procedures are designed to attain the best optimal value. Therefore, optimization using the WOA has been proposed to segment the brain's inner regions. However, it has drawbacks in identifying search agents (SAs) for obtaining the optimal solution. Hence, the presented work concentrated on a hybrid of the WOA and GWO to achieve an accurate solution.

3.3.1. Whale Optimization Algorithm (WOA)

The WOA is a well-known optimization approach for solving complicated issues. It contains three operators: searching for prey, enclosing prey, and the bubble-net foraging behavior of humpback whales. Bubble-net foraging, which uses separate bubbles, is a unique method of hunting. The WOA's hunting process is outlined as follows. Encircling prey: Over multiple cycles, humpback whales encircle their prey and update their positions

until they achieve the optimal solution [34]. The main aim of bubble-net foraging is to identify the subregions of the brain (this will be called the hunting of subregions) in terms of obtaining the optimized solution.

The prey can be attacked by humpback whales using the spiral bubble-net approach, which is described in the following. The shrinkage of the encircling mechanism is used to decrease the coefficient vector A_1 :

$$A_1 = 2a_1 \cdot r1 - a_1,$$

where $r1$ is a random number between 0 and 1.

Updating the spiral position: The motion of humpbacks is mathematically stated as follows:

$$X_1(n + 1) = D'_1 * e^{bv} * \cos(2\pi v) + X_1(n), \quad D_1 = |X_1(n) - X'_1(n)|,$$

where v is a random number, b is a constant (it determines the spiral's form), X'_1 is the vector of the prey's location, and X_1 is the humpback whales' location vector. Generally, humpback whales roam within the circle of prey in their spiral path. Then, the probability of selecting the spiral model or encircling mechanism is updated with the following equation:

$$X_1(n + 1) = \begin{cases} X'_1(n) - A_1 * D_1 & \text{if } p_1 < 0.5 \\ D'_1 * e^{bv} * \cos(2\pi v) + X'_1(n), & \text{if } p_1 < 0.5 \end{cases}$$

where p_1 is a random value within [0, 1].

Searching for prey: Prey is searched for randomly by humpback whales. The location of the whale is updated by using a random search agent and then the best search agent, which is described below:

$$D_1 = |C_1 * X_{rand} - X_1|, \quad X_1(n + 1) = X_{rand} - A_1 * D_1, \quad X_{rand} :$$

which is the random position vector selected from the current position [26,34,35].

3.3.2. Gray Wolf Optimization (GWO)

GWO is a metaheuristic algorithm that applies a special leadership quality to the hunting mechanism [34]. The mathematical process of GWO involves the societal hierarchy, encircling prey, searching for prey, and hunting and attacking prey, which is discussed in the following.

Societal hierarchy: The leader wolves are alpha (α), which is the first level. Similarly, the second- and third-level wolves are beta (β) and delta (δ).

Encircling prey: Prey is encircled by gray wolves during hunting (D_1), which is mathematically represented by the following formulas [34]:

$$D_1 = |C_1 * X_p(n) - X_1(n)|, \quad X_1(n + 1) = X_p(n) - A_1 D_1$$

where X_p is the prey position vector, n is the current iteration, X_1 is the gray wolf position vector, and A_1 and C_1 are coefficient vectors [34].

$$A_1 = 2a_1 \cdot r1 - a_1, \quad C_1 = 2 * r2,$$

where $r1$ and $r2$ are random numbers between 0 and 1.

Hunting: The mathematical process of hunting is defined below [34]:

$$D1_\alpha = |C_1 * X_\alpha - X|, \quad D1_\beta = |C_2 * X_\beta - X|, \quad D1_\delta = |C_3 * X_\delta - X|,$$

$$X_1 = X_\alpha - A_3 * d_\alpha, \quad X_2 = X_\beta - A_3 * d_\beta, \quad X_3 = X_\delta - A_3 * d_\delta,$$

where X_α , X_β , and X_δ are the α (alpha), β (beta), and δ (delta) gray wolves' positions [38].

Finally, the positions of the SAs can be updated by using the following formula [35,39]:

$$X(n+1) = \frac{X_1 + X_2 + X_3}{3}$$

Attacking the prey: If $|A| < 1$, the wolves move toward the prey to attack. Searching for prey: If $|A| > 1$, the wolves move away from the prey for filtering [34].

3.3.3. Hybrid WOA and GWO

The presented work implemented a hybrid of the WOA and GWO to improve the performance of the WOA. The improvements were achieved by the leadership characteristic of GWO and were applied to the WOA bubble-net strategy. Because of its natural aptitude for hunting, GWO picks the three best options, such as alpha, beta, and delta, which are utilized in the WOA exploitation stage to adjust the SA's location and improve the WOA's performance [34]. Bubble-net attacking process: The proposed hybrid method updates the positions of the whales using the natural leadership behavior of GWO by using a mathematical representation, which is given below [34,35]. Shrinking encircling mechanism: The positions of humpback whales are updated with the following: $X(n+1) = \frac{X_1 + X_2 + X_3}{3}$ [26,34]. Updating the spiral position: The humpback whales' positions are updated along with a spiral-shaped path, which is given below [26,34]:

$$D1'_{\alpha} = |C_1 * X_{\alpha} - X|, \quad D1'_{\beta} = |C_2 * X_{\beta} - X|, \quad D1'_{\delta} = |C_3 * X_{\delta} - X|$$

$$X_1(n) = X_{\alpha}(n) + D'_{\alpha} * e^{bv} * \cos(2\pi v),$$

$$X_2(n) = X_{\beta}(n) + D'_{\beta} * e^{bv} * \cos(2\pi v)$$

$$X_3(n) = X_{\delta}(n) + D'_{\delta} * e^{bv} * \cos(2\pi v)$$

$$X(n+1) = \frac{X_1 + X_2 + X_3}{3}$$

Pseudocode for the proposed hybrid algorithm (Algorithm 1):

Algorithm 1. Pseudocode

S1: Initial population of the SA has been generated
 S2: Determine the fitness function for each search agent.
 S3: X_{α} : first best solution
 S4: X_{β} : second best solution
 S5: X_{δ} : third best solution
 S6: if1 $n < \text{max no. of iterations}$
 S7: for $i = 1$ to no. of search agent
 S8: update the parameters of A, C, a, l , and p
 S9: if2 ($p1 < 0.5$)
 S10: if3 ($|A| < 1$)
 S11: search agent position has been updated.
 S12: else if3 ($|A| \geq 1$)
 S13: random agent selection (X_{rand}) and update the search agent position.
 S14: end if3
 S15: else if2 ($p1 \geq 0.5$) and update the position of the search agent.
 S16: end if2
 S17: checks the search agent position whether it has gone outside of the assigned search space.
 S18: positions of $X_{\alpha}, X_{\beta}, X_{\delta}$ are updated.
 S19: update the number of iterations
 S20: end if
 S21: Return X_{α}

3.3.4. Ground-Truth Validation

Quality evaluation methodologies, including Feature Similarity Index Metrics and Structure Similarity Index Metrics, have been utilized to determine the validity of the similarity between GT and SR [39,40].

3.4. Classification

Deep learning (DL) is used for deep classification, which is also part of machine learning (ML). The input and output layers of DL have a standard topology, with hidden layers oriented toward the network architecture. The basic purpose of choosing a DL classifier is to obtain extremely high classification performance. One of the basic DL architectures is the Convolution Neural Network (CNN), which consists of many layers for visual feature extraction and classification [20]. The Convolution Neural Network (CNN), which has many layers and is the main DL network, is used to classify and reduce the number of features in images. In order to complete feature extraction and classification, this work focused on the CNN. This network has a large number of convolutional filters that extract image features. This work used AlexNet for feature extraction and classification, which aids in the categorization of NC and AD patients because of its various convolution filters that extract visual characteristics. Sensitivity, accuracy, and specificity are calculated as outcomes of the classification, as are statistical measures such as true positive (TP), false negative (FN), true negative (TN), and false positive (FP) rates. These measurements also compute the recall, accuracy, and F-score in order to assess the performance of the proposed approach in Alzheimer's disease prediction [38].

3.5. Clinical Score Validation

The MMSE is a type of test used to assess neurobiological and physical disabilities. The MMSE score and patient history report are required for the appropriate medical evaluation to classify NC and AD patients [41]. It is used for cognitive screening, which offers grading based on impairment, and it has become the standard test for monitoring the phases of Alzheimer's disease. The MMSE is made up of eleven questions that cover six cognitive functions: short-term recollection, language, immediate recall, attention, and the ability to track basic verbal and written directions. The suggested approach for determining the association between the SR and cognitive functions involves comparing the MMSE to the SR intensity value. The MMSE score typically ranges from 0 to 30 points and declines as the condition progresses. NC is defined as a score between 26 and 30, whereas AD is defined as a score less than or equal to 18 [42]. Mild cognitive impairment is indicated by a score between 18 and 24 (MCI).

4. Results and Discussion

Initially, images for both NC and AD patients were obtained from Chettinad Hospital. Based on the doctor's contribution, this study took into account around 200 images from real-time public databases. AD is a neurological/neuropathological illness that affects brain structures and produces a variety of cognitive impairments, including increased confusion, loss of knowledge, impairment in memory skills, and difficulties comprehending and performing activities. As a result, there is a need to focus on the brain's interior areas, such as the ventricle, CC, GM, HC, and WM, when analyzing AD. The suggested system considers all three slices (axial, coronal, and sagittal) of the encephalon/brain to segment all of the above-mentioned areas. Figure 2 shows the raw pictures of all three slices of NC and AD images. Because of anatomical differences, the encephalon's inner tissues are very small and difficult to distinguish. Because the interior parts of the brain have undefined borders and have relatively low contrast, they must be preprocessed.

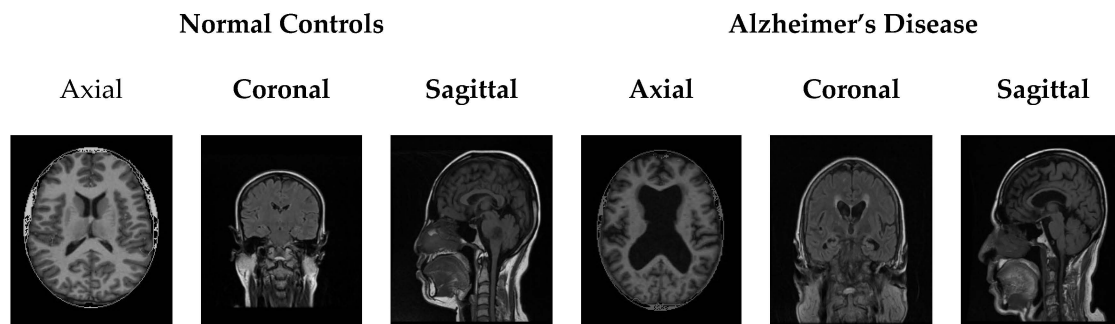


Figure 2. Input images of NC and AD with different slices.

To identify the target region of the brain, preprocessing steps such as skull stripping and contrast enhancement were conducted to produce good-quality images. Otsu's thresholding was used in skull stripping to eliminate non-brain tissues from input images, such as the fat, scalp, muscle, skull, and skin. Similarly, histogram equalization was applied in order to preserve information with high contrast. Figure 3 shows the preprocessed images.

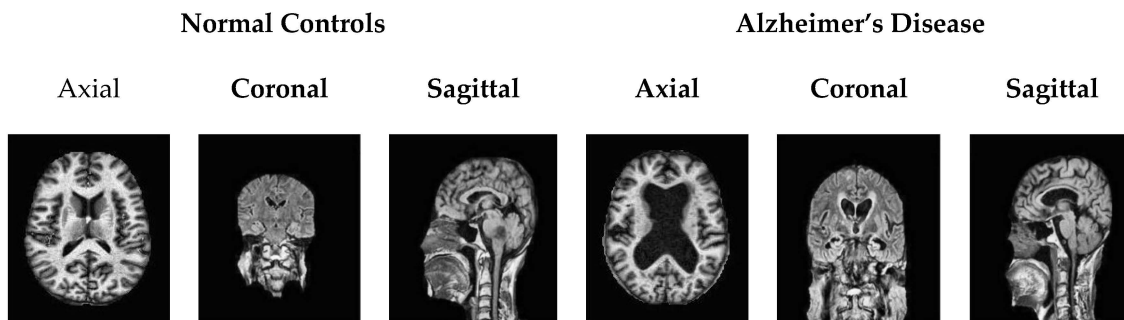


Figure 3. Preprocessed images of NC and AD.

Implementation of Hybrid Technique

Generally, the segmentation of brain regions is a problematic process since the brain has a compound structure. Hence, the presented work started with the implementation of the WOA method for segmenting the brain's inner regions, which are the ventricle, GM, CC, WM, and HC. The WOA has two phases of hunting: exploitation and exploration. The WOA employs the bubble-net attack tactic for hunting during the exploitation stage. Though the conventional whale optimization algorithm produces the best results in some cases, this technique may rely on the local optimal solution. As a result, in order to address this issue, a hybrid of the WOA and GWO (HWGO) was developed for the segmentation process in order to enhance the hunting exploitation process. In the suggested system, GWO's management and leadership qualities may be exploited in the WOA's bubble-net hunting approach. Throughout the WOA exploitation stage, the proposed algorithm selects the three best solutions from all (combination of the WOA and GWO) search agents, and other SAs adjust their locations based on their positions.

The major parameters of the WOA and HWGO are the number of search agents, number of iterations, and number of threshold values, which are listed in Table 2. The process of fitness function evaluation is repeated until it reaches the best solution. The ending criteria were set to the number of iterations (I) and the number of thresholds (T1). These parameters were experimentally tuned quantitatively and qualitatively to achieve the best solution for segmenting all of the above-mentioned regions. The qualitative measures specify that if the value of T is small, then the SR also includes neighborhood pixels. Similarly, when the value of T is large, the SR regions are blurred. Finally, we obtained the T values for the GM, CC, WM, ventricle, and HC, which were 5, 10, 5, 8, and 13, respectively. Then, the next parameter designated for selecting the optimal value is the number of SAs, and it

was fixed at 100 for segmentation. The segmented brain’s inner regions, especially the GM, ventricle, CC, HC, and WM, are presented in Figures 4–8 for the different optimization techniques. The segmented output clearly shows the qualitative performance of the WOA and HWGO for various regions. According to Figures 4–8, the regions can be segmented more accurately with HWGO than with the WOA due to its quality of searching for the global solution. Based on the qualitative analysis, it is demonstrated that the WOA displays very low performance compared to HWGO due to its naturally poor encircling (bubble-net attack) mechanism during hunting.

Table 2. The optimal values for the proposed algorithms.

Parameters	WOA					HWGO				
	Ven	GM	WM	CC	HC	Ven	GM	WM	CC	HC
No. of SAs	100	100	100	100	100	100	100	100	100	100
I	100	100	100	100	100	100	100	100	100	100
T1	8	5	5	10	13	8	5	5	10	13

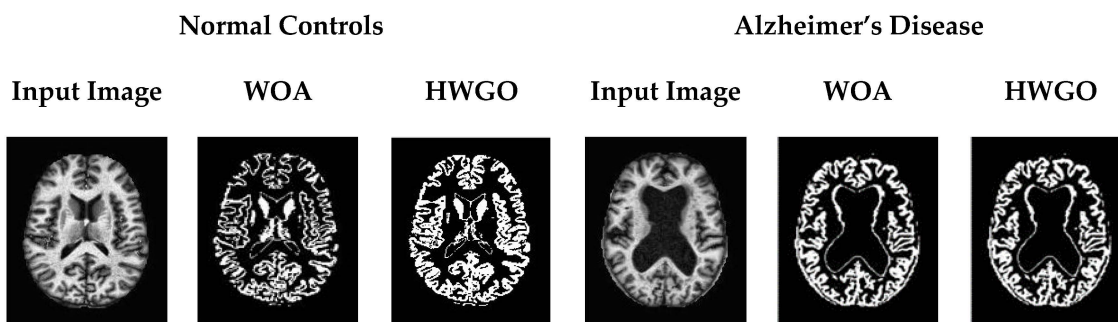


Figure 4. Segmentation of GM using WOA and HWGO.

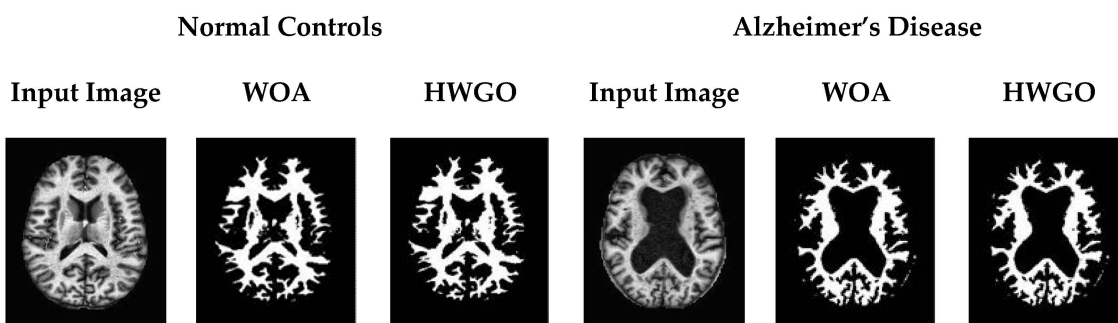


Figure 5. Segmentation of WM using WOA and HWGO.

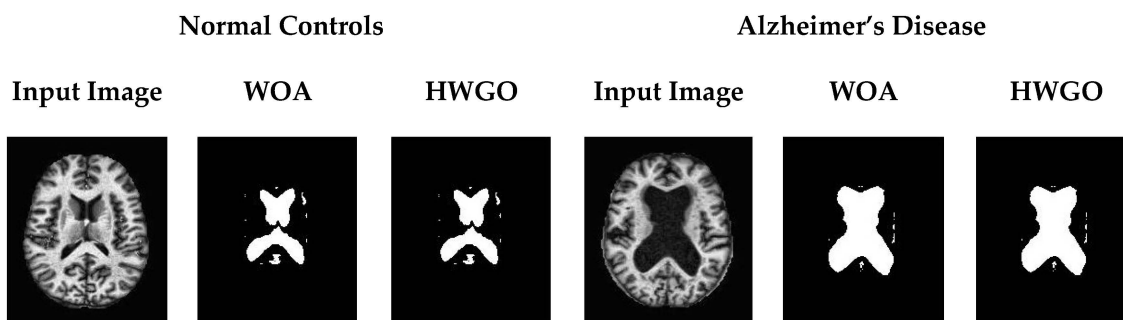


Figure 6. Segmentation of ventricle using WOA and HWGO.

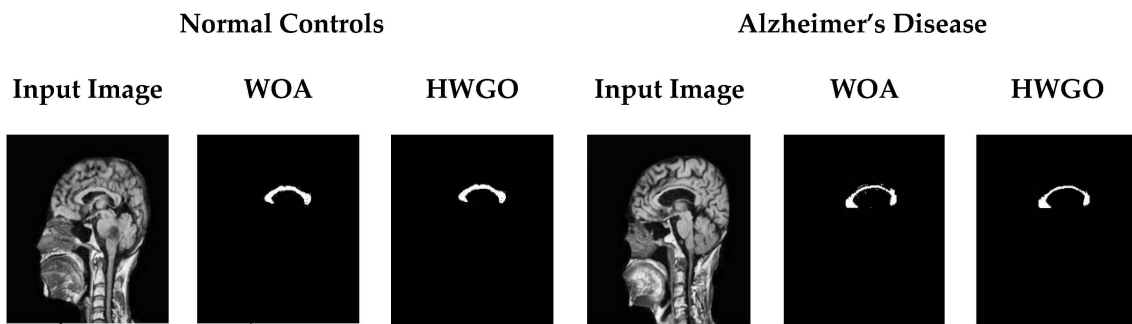


Figure 7. Segmentation of CC using WOA and HWGO.

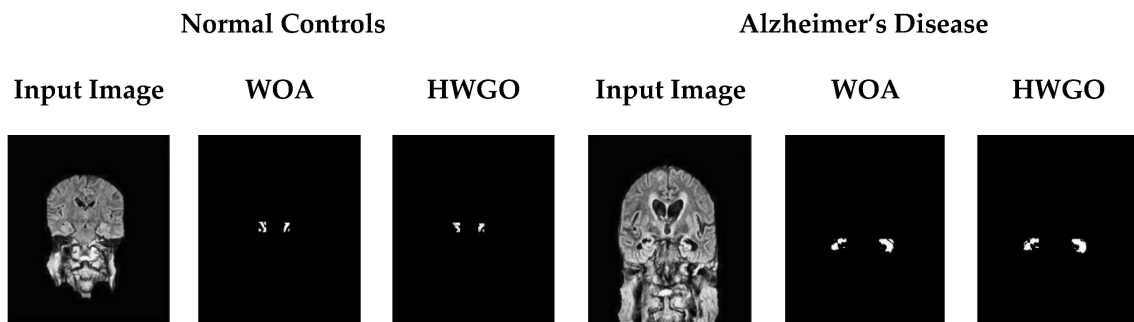
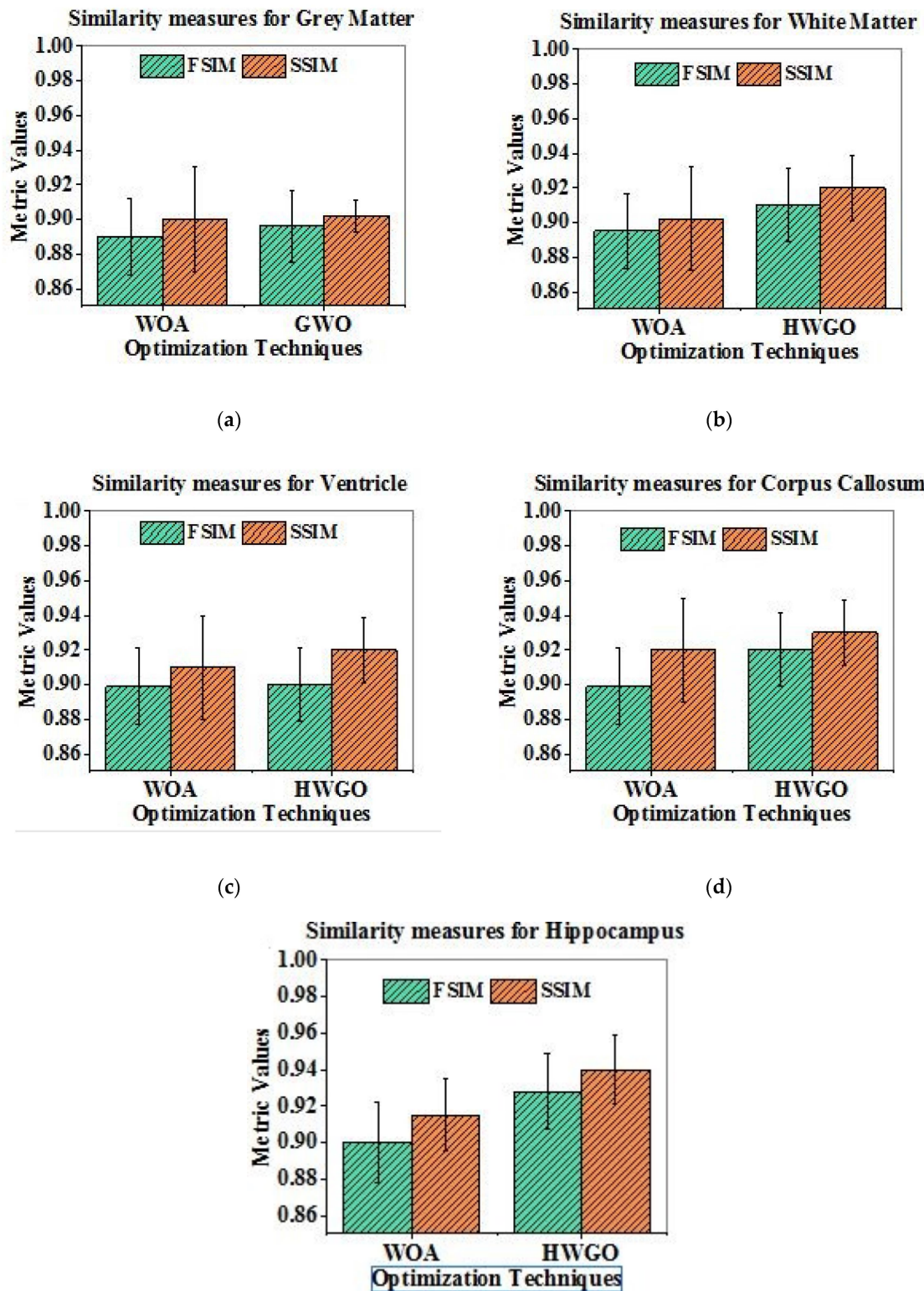


Figure 8. Segmentation of HC using WOA and HWGO.

The parameter values are finalized with the quantitative analysis of GT and SR images. The GT images were collected from Chettinad Hospital with the approval of the doctors. After the segmentation operation, the SR results were validated using GT pictures and numerous performance indicators, including FSIM and SSIM. These metrics serve to establish the comparability of GT and SR based on image properties and structure. In the same way, these measures reveal the accuracy of the segmentation results for NC and AD. The measures were calculated for the brain's five inner regions with the WOA and the hybrid of the WOA and GWO. These measures clearly illustrate the improvement of the WOA in hybrid segmentation due to the implementation of GWO in the WOA. GWO provides better support in identifying the best solution in terms of finding the three best solutions during the encircling mechanism. Similarly, HWGO improves the performance of the WOA due to its combination with GWO in finding the similarity between the SR and GT of the brain's inner regions. Finally, the accuracy of HWGO is 94% in both the FSIM and SSIM for the HC, GM, ventricle, WM, and CC. This proves that the segmentation performance of the WOA is improved since GWO enhances the reliability and quantitative performance of the WOA in HWGO (Figure 9). The suggested technique (HWGO) outperforms the WOA in the segmentation of the GM, ventricle, WM, CC, and HC because it features an encircling mechanism that finds the best results. In comparison, the suggested method shows increased performance because it shows the highest similarity between the SR and GT regions of the GM, ventricle, CC, WM, and HC. It has a significantly higher FSIM and SSIM accuracy of 94 percent compared to the WOA (Figure 9). Table 3 displays the accuracy, sensitivity, and specificity of GT and SR, which are utilized to categorize normal control and AD pictures using the DL classifier. Based on these measures, it is observed that both segmentation and classification showed better optimal solutions in the hybrid method, and it improves the exploration and exploitation levels of the individual method. Finally, the presented work applied the Mini-Mental Score Evaluation to compare the results with the clinical status.



(a) (b) (c) (d) (e)

Figure 9. Similarity measures: (a) gray matter, (b) white matter, (c) ventricle, (d) corpus callosum, (e) hippocampus.

Table 3. Statistical measures using GT and segmented hippocampus.

Statistical Measures	WOA	HWGO	WOA	HWGO	WOA	HWGO	WOA	HWGO	WOA	HWGO
	GM		WM		Ventricle		CC		HC	
Accuracy	0.88	0.91	0.89	0.91	0.89	0.91	0.912	0.934	0.92	0.94
Sensitivity	0.89	0.90	0.89	0.90	0.89	0.90	0.90	0.915	0.90	0.93
Specificity	0.88	0.90	0.88	0.90	0.88	0.90	0.91	0.91	0.91	0.91

Figure 10 depicts the association between the pixel intensity and MMSE score in the HC area. The normal pixel intensity of the HC region is between 91 and 94, whereas that of Alzheimer’s disease is between 81 and 85. From the results of this validation, the structural anomalies of normal and Alzheimer’s disease patients are assessed using the MMSE score. The graph clearly shows that the MMSE score in both normal and AD patients is highly related to the number of intensity values. As a result, the data collected are therapeutically useful, and they might be utilized to screen Alzheimer’s patients. According to the segmentation and classification results, the HC area is a responsible/key region for identifying an abnormal image of a patient. Hence, the MMSE score was examined for the HC region to differentiate between AD and normal controls, the result of which is shown in Figure 10.

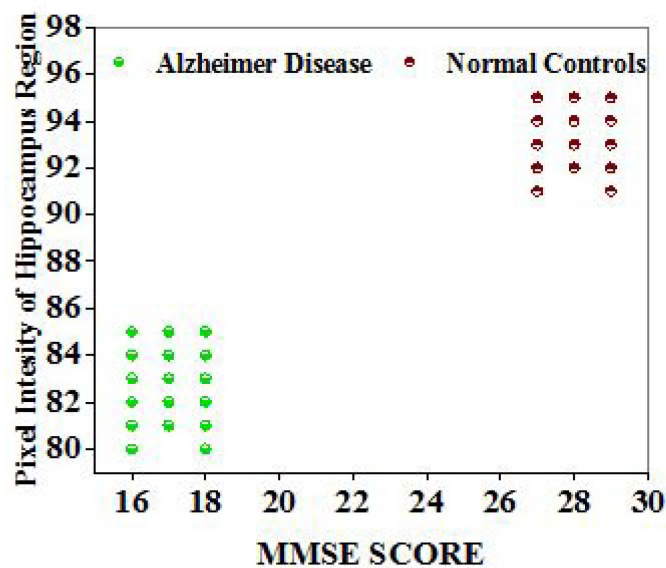


Figure 10. Mini-Mental Examination Score comparison with GT and SR.

Computational complexity was calculated with the number of iterations and the fitness value. The number of iterations is taken as a major factor in attaining the optimal solution. The convergence characteristic graph for segmenting internal brain regions in AD and normal images using the WOA and the HWGO algorithm. The graph was created by plotting the number of iterations against the fitness score. For the optimization techniques described above, the maximum number of iterations was set at 100. Table 4 demonstrates that the HWGO method is more stable in reaching global optimal solutions with fewer iterations.

Table 4. Computational complexity of the proposed optimization algorithm.

Optimization Algorithm	WOA	GWO	HWGO
Number of iterations to attain optimal solutions/maximum number of iterations	82/100	62/100	75/100
Time complexity	30.425	23.782	26.782

Generally, region extraction from the brain is more sensitive, and it is a more challenging task in identifying/classifying disease progression. However, it is very difficult. It is necessary to identify and extract individual regions to analyze major diseases, such as dementia, brain cancer, AD, epilepsy, and others. As a result, various authors have proposed various methods, such as Fuzzy C means, GWO, BAT, ABC, WDO, and so on, for brain disease progression and have shown better outcomes [43–50]. According to Table 5, the highest performance was shown by HWGO compared to other methods. According to the findings, the HC provides more signals for diagnosing atrophy in all situations. The atrophy of the HC has a substantial influence on memory. According to the study, the hippocampal region is the most impacted region in the early stages of Alzheimer’s disease compared to other areas since it is located deep inside the brain; it is important for memory assessments, and it is used as a predictive marker for studying the disease. Similarly, the proposed strategy emphasizes the significance of the HC sector.

Table 5. Comparison between existing and proposed techniques.

Authors	Selected Regions	Accuracy %
Pang et al. [47]	HC	87.7
Singh and Bala [48]	WM, GM, CSF	91.7
Pham et al. [10]	WM, GM, CSF	92.9
Proposed techniques	GM, CC, ventricle, WM and HC	94

5. Conclusions

The most difficult process in diagnosing illness progression is the segmentation of brain areas such as the ventricle, GM, CC, WM, and HC. This research focuses on brain subregion segmentation in order to identify Alzheimer’s disease and normal controls. Initially, this work started with data collection from Chettinad Hospital. Then, it moved on to preprocessing for contrast enhancement and skull stripping. Next, the segmentation and classification process was performed using the WOA and HWGO. Quantitative and qualitative analyses such as similarity measures, statistical measures, and clinical score validation were conducted by calculating the FSIM, SSIM, accuracy, sensitivity, and specificity for the optimal solution. Initially, this work was performed for five regions, specifically the GM, ventricle, CC, HC, and WM. As per clinical and experimental outcomes, the HC region is more suitable and responsible for the diagnosis. Thus, the HC area was quantified using two optimization approaches (WOA and HWGO) and DL, which were utilized to diagnose AD and NC. In general, the hospital images were of low quality. As a result, an attempt was made to improve image quality by adopting preprocessing techniques. This work combined the WOA with GWO to enhance the outcomes of the WOA. Based on this validation, HWGO delivered a maximum accuracy of 92 percent in segmentation when compared to other approaches since it has the capacity of a leader to pick the optimal solution. Because GWO accurately isolates genuine areas of brain subregions, the GWO approach was used with the WOA to assess the performance of the WOA. GWO demonstrated improvements and provided a superior solution in this hybridization. The results show that 94 percent of the data match GT. After classification validation, MMSE validation was also conducted to clinically prove the method’s performance using experimental values. According to the data, the proposed task successfully showed the best outcome. The suggested technique

is beneficial for screening systems and as a research tool for neurodegenerative diseases, namely, Alzheimer's disease.

Author Contributions: Conceptualization, C.D. and S.K.M. (Sathish Kumar Mani); methodology, S.K.M. (Sandeep Kumar Mathivanan); validation, P.J.; resources, S.M. (Senthilkumar Mohan); data curation, S.M. (Saurav Mallik); writing—original draft preparation, C.D. and S.K.M. (Sathish Kumar Mani); writing—review and editing, S.K.M. (Sandeep Kumar Mathivanan) and P.J.; visualization, H.Q.; supervision, P.J., S.M. (Senthilkumar Mohan), S.M. (Saurav Mallik), and H.Q.; project administration, P.J., S.M. (Senthilkumar Mohan), S.M. (Saurav Mallik), and H.Q. All authors have read and agreed to the published version of the manuscript.

Funding: H.Q. is grateful for USA NSF awards 1761839 and 2200138 and a catalyst award from the USA National Academy of Medicine.

Institutional Review Board Statement: Not applicable.

Informed Consent Statement: Not applicable.

Data Availability Statement: Not applicable.

Conflicts of Interest: The authors declare no conflict of interest.

References

1. Alzheimer's Association. Available online: <https://www.alz.org/in/dementia-alzheimers-en.asp> (accessed on 1 March 2019).
2. Dementia Australia 2002. Available online: <https://www.dementia.org.au/about-dementia/types-of-dementia/alzheimers-disease> (accessed on 1 July 2016).
3. Brunnström, H.; Englund, E. Comparison of four neuropathological scales for Alzheimer's disease. *Clin. Neuropathol.* **2011**, *30*, 56–69. [[CrossRef](#)]
4. Serrano-Pozo, A.; Frosch, M.P.; Masliah, E.; Hyman, B.T. Neuropathological Alterations in Alzheimer Disease. *Cold Spring Harb. Perspect. Med.* **2011**, *1*, a006189. [[CrossRef](#)]
5. Thal, D.R.; Rüb, U.; Orantes, M.; Braak, H. Phases of A β -deposition in the human brain and its relevance for the development of AD. *Neurology* **2002**, *58*, 1791–1800. [[CrossRef](#)]
6. Arakeri, M.P.; Reddy, G.R.M. Computer-aided diagnosis system for tissue characterization of brain tumor on magnetic resonance images. *Signal Image Video Process.* **2013**, *9*, 409–425. [[CrossRef](#)]
7. Bhandari, A.K.; Singh, V.K.; Kumar, A.; Singh, G.K. Cuckoo search algorithm and wind driven optimization based study of satellite image segmentation for multilevel thresholding using Kapur's entropy. *Expert Syst. Appl.* **2014**, *41*, 3538–3560. [[CrossRef](#)]
8. Holl, J.H. Genetic algorithms. *Sci. Am.* **1992**, *267*, 66–73.
9. Kennedy, J.; Eberhart, R. Particle Swarm Optimization. In Proceedings of the ICNN'95—International Conference on Neural Networks, Perth, Australia, 27 November–1 December 1995; Volume 4, pp. 1942–1948. [[CrossRef](#)]
10. Pham, T.X.; Siarry, P.; Oulhadj, H. An improved particle swarm optimization algorithm for MRI image segmentation. In Proceedings of the 13th Biennial International Conference on Artificial Evolution, Artificial Evolution, Paris, France, 25–27 October 2017; pp. 277–284.
11. Cao, X.; Miao, J.; Xiao, Y. Medical Image Segmentation of Improved Genetic Algorithm Research Based on Dictionary Learning. *World J. Eng. Technol.* **2017**, *5*, 90–96. [[CrossRef](#)]
12. Mirjalili, S. The Ant Lion Optimizer. *Adv. Eng. Softw.* **2015**, *83*, 80–98. [[CrossRef](#)]
13. Mirjalili, S.; Lewis, A. The Whale Optimization Algorithm. *Adv. Eng. Softw.* **2016**, *95*, 51–67. [[CrossRef](#)]
14. Mirjalili, S. Moth-flame optimization algorithm: A novel nature-inspired heuristic paradigm. *Knowl. Based Syst.* **2015**, *89*, 228–249. [[CrossRef](#)]
15. Mirjalili, S. Dragonfly algorithm: A new meta-heuristic optimization technique for solving single-objective, discrete, and multi-objective problems. *Neural Comput. Appl.* **2016**, *27*, 1053–1073. [[CrossRef](#)]
16. Dorgham, O.M.; Alweshah, M.; Ryalat, M.H.; Alshaer, J.; Khader, M.; Alkhalaleh, S. Monarch butterfly optimization algorithm for computed tomography image segmentation. *Multimed. Tools Appl.* **2021**, *80*, 30057–30090. [[CrossRef](#)]
17. Lin, S.; Jia, H.; Abualigah, L.; Altalhi, M. Enhanced Slime Mould Algorithm for Multilevel Thresholding Image Segmentation Using Entropy Measures. *Entropy* **2021**, *23*, 1700. [[CrossRef](#)] [[PubMed](#)]
18. Alagarsamy, S.B.; Murugan, K. Ear recognition system using adaptive approach Runge-Kutta (AARK) threshold segmentation with cart classifier. *Multimed. Tools Appl.* **2019**, *79*, 10445–10459. [[CrossRef](#)]
19. Saidala, R.K.; Devarakonda, N. Improved Whale Optimization Algorithm Case Study: Clinical Data of Anaemic Pregnant Woman. In *Data Engineering and Intelligent Computing*; Springer: Cham, Switzerland, 2018.
20. Mohsen, H.; El-Dahshan, E.-S.A.; El-Horbaty, E.-S.M.; Salem, A.-B.M. Classification using deep learning neural networks for brain tumors. *Future Comput. Inform. J.* **2018**, *3*, 68–71. [[CrossRef](#)]
21. Pressman, P.; Rabinovici, G. Alzheimer's Disease. *Encycl. Neurol. Sci.* **2014**, 122–127. [[CrossRef](#)]
22. Blennow, K.; de Leon, M.J.; Zetterberg, H. Alzheimer's disease. *Lancet* **2006**, *368*, 387–403. [[CrossRef](#)]

23. Puthiyedth, N.; Riveros, C.; Berretta, R.; Moscato, P. Identification of Differentially Expressed Genes through Integrated Study of Alzheimer's Disease Affected Brain Regions. *PLoS ONE* **2016**, *11*, e0152342. [[CrossRef](#)] [[PubMed](#)]
24. Frisoni, G.; Beltramello, A.; Weiss, C.; Geroldi, C.; Bianchetti, A.; Trabucchi, M. Linear measures of atrophy in mild Alzheimer disease. *Am. J. Neuroradiol.* **1996**, *17*, 913–923. [[PubMed](#)]
25. Villain, N.; Desgranges, B.; Viader, F.; de la Sayette, V.; Mezenge, F.; Landeau, B.; Baron, J.-C.; Eustache, F.; Chetelat, G. Relationships between Hippocampal Atrophy, White Matter Disruption, and Gray Matter Hypometabolism in Alzheimer's Disease. *J. Neurosci.* **2008**, *28*, 6174–6181. [[CrossRef](#)] [[PubMed](#)]
26. Singh, N.; Hachimi, H. A New Hybrid Whale Optimizer Algorithm with Mean Strategy of Grey Wolf Optimizer for Global Optimization. *Math. Comput. Appl.* **2018**, *23*, 14. [[CrossRef](#)]
27. Passino, K.M. Biomimicry of bacterial foraging for distributed optimization and control. *IEEE Control Syst. Mag.* **2002**, *22*, 52–67. [[CrossRef](#)]
28. Holland, J.H. *Adaptation in Natural and Artificial Systems*, 1st ed.; University of Michigan Press: Ann Arbor, MI, USA, 1975.
29. Karaboga, D.; Basturk, B. On the performance of artificial bee colony (ABC) algorithm. *Appl. Soft Comput.* **2008**, *8*, 687–697. [[CrossRef](#)]
30. El Aziz, M.A.; Ewees, A.A.; Hassanien, A.E. Whale Optimization Algorithm and Moth-Flame Optimization for multilevel thresholding image segmentation. *Expert Syst. Appl.* **2017**, *83*, 242–256. [[CrossRef](#)]
31. Dorigo, M. Ant colony optimization. *Scholarpedia* **2007**, *2*, 1461. [[CrossRef](#)]
32. Yang, X.-S.; Deb, S. Cuckoo Search via Levy flights. In Proceedings of the 2009 World Congress Nature & Biologically Inspired Computing (NaBIC), Coimbatore, India, 9–11 December 2009; pp. 210–214. [[CrossRef](#)]
33. Gharehchopogh, F.S. A comprehensive survey: Whale Optimization Algorithm and its applications. *Swarm Evol. Comput.* **2019**, *48*, 1–24. [[CrossRef](#)]
34. Korashy, A.; Kamel, S.; Jurado, F.; Youssef, A.-R. Hybrid Whale Optimization Algorithm and Grey Wolf Optimizer Algorithm for Optimal Coordination of Direction Overcurrent Relays. *Electr. Power Components Syst.* **2019**, *47*, 644–658. [[CrossRef](#)]
35. Xiao, Z.; Ding, Y.; Lan, T.; Zhang, C.; Luo, C.; Qin, Z. Brain MR Image Classification for Alzheimer's Disease Diagnosis Based on Multifeature Fusion. *Comput. Math. Methods Med.* **2017**, *2017*, 1–13. [[CrossRef](#)]
36. Jo, T.; Nho, K.; Saykin, A.J. Deep Learning in Alzheimer's Disease: Diagnostic Classification and Prognostic Prediction Using Neuroimaging Data. *Front. Aging Neurosci.* **2019**, *11*, 220. [[CrossRef](#)]
37. Haq, A.U.; Li, J.P.; Khan, S.; Alshara, M.A.; Alotaibi, R.M.; Mawuli, C. DACBT: Deep learning approach for classification of brain tumors using MRI data in IoT healthcare environment. *Sci. Rep.* **2022**, *12*, 15331. [[CrossRef](#)]
38. Chitradevi, D.; Prabha, S. Analysis of brain sub regions using optimization techniques and deep learning method in Alzheimer disease. *Appl. Soft Comput.* **2019**, *86*, 105857. [[CrossRef](#)]
39. Suresh, S.; Lal, S. An efficient cuckoo search algorithm based multilevel thresholding for segmentation of satellite images using different objective functions. *Expert Syst. Appl.* **2016**, *58*, 184–209. [[CrossRef](#)]
40. Suganthi, S.; Ramakrishnan, S. Anisotropic diffusion filter based edge enhancement for segmentation of breast thermogram using level sets. *Biomed. Signal Process. Control.* **2014**, *10*, 128–136. [[CrossRef](#)]
41. Vemuri, P.; Jones, D.T.; Jr, C.R.J. Resting state functional MRI in Alzheimer's Disease. *Alzheimer's Res. Ther.* **2012**, *4*, 1–9. [[CrossRef](#)] [[PubMed](#)]
42. Cao, L.; Li, L.; Zheng, J.; Fan, X.; Yin, F.; Shen, H.; Zhang, J. Multi-task neural networks for joint hippocampus segmentation and clinical score regression. *Multimed. Tools Appl.* **2018**, *77*, 29669–29686. [[CrossRef](#)]
43. Prabha, S.; Sankaran, K.; Chitradevi, D. Efficient optimization based thresholding technique for analysis of alzheimer MRIs. *Int. J. Neurosci.* **2021**, *133*, 201–214. [[CrossRef](#)]
44. Chitradevi, D.; Prabha, S.; Prabhu, A.D. Diagnosis of Alzheimer disease in MR brain images using optimization techniques. *Neural Comput. Appl.* **2020**, *33*, 223–237. [[CrossRef](#)]
45. Chitradevi, D.; Prabha, S. Analysis of Alzheimer Disease using Optimization Techniques. In Proceedings of the 2020 Sixth International Conference on Bio Signals, Images, and Instrumentation (ICBSII), Chennai, India, 27–28 February 2020; pp. 1–5. [[CrossRef](#)]
46. Chitradevi, D.; Prabha, S.; Sankaran, K. Brain Hemisphere Analysis Using Genetic Algorithm and Fuzzy Clustering in Alzheimer Disease. In Proceedings of the 2018 International Conference on Communication and Signal Processing (ICCSP), Chennai, India, 3–5 April 2018; pp. 901–905. [[CrossRef](#)]
47. Pang, S.; Jiang, J.; Lu, Z.; Li, X.; Yang, W.; Huang, M.; Zhang, Y.; Feng, Y.; Huang, W.; Feng, Q. Hippocampus Segmentation Based on Local Linear Mapping. *Sci. Rep.* **2017**, *7*, 45501. [[CrossRef](#)]
48. Singh, C.; Bala, A. A DCT-based local and non-local fuzzy C-means algorithm for segmentation of brain magnetic resonance images. *Appl. Soft Comput.* **2018**, *68*, 447–457. [[CrossRef](#)]

49. Meng, L.; Xiang, J. Brain Network Analysis and Classification Based on Convolutional Neural Network. *Front. Comput. Neurosci.* **2018**, *12*, 95. [[CrossRef](#)]
50. Ždímalová, M.; Chatterjee, A.; Kosnáčová, H.; Ghosh, M.; Obaidullah, S.M.; Kopáni, M.; Kosnáč, D. Various Approaches to the Quantitative Evaluation of Biological and Medical Data Using Mathematical Models. *Symmetry* **2021**, *14*, 7. [[CrossRef](#)]

Disclaimer/Publisher's Note: The statements, opinions and data contained in all publications are solely those of the individual author(s) and contributor(s) and not of MDPI and/or the editor(s). MDPI and/or the editor(s) disclaim responsibility for any injury to people or property resulting from any ideas, methods, instructions or products referred to in the content.